Asian Journal of Information Technology 6 (3): 268-273, 2007

Design of Three-Phase and Four-Phase LSRM with Active Stator and Passive Translator of the Linear Switched Reluctance Machine

Abdelkamel Dekhinet, Cherif Fetha and Khaled Chikhi
Faculty of Sciences Engineering, University of Batna,
Rue Chahid Med Elhadi Boukhlouf, 05000 Batna, Algeria

Abstract: A standard design procedure for a single-sided and longitudinal-flux-based Linear Switched Reluctance Machine (LSRM) is developed in this section. The proposed design procedure utilizes the rotating Switched Reluctance Machine (rotary SRM) design by converting the specifications of the linear machine into those of an equivalent rotating machine. The machine design is carried out in the rotary domain, which then is transformed back into the linear domain. Such a procedure brings to bear the knowledge base and familiarity of the rotary machine designers to design a linear machine effectively. This study contains illustrations of the proposed design procedure for a three-phase LSRM with an active stator and passive translator and a four-phase LSRM with an active translator and passive stator. Analysis procedures for the phase winding inductance and propulsion and normal forces vs. translator position are developed with a lumped-parameter magnetic circuit model. The results from it are verified with finite element analysis. The experimental setup for measurements of inductance vs. position vs. current, propulsion force vs. position vs. current and normal force vs. position vs. current is described.

Key words: Magnetic circuit model, design of a linear switched reluctance motor, synchronous reluctance motor

INTRODUCTION

There are two distinct configurations of LSRM: Transverse flux and longitudinal flux. Transverse flux machines have been explored in detail in the literature; however, the design of machines is not described in detail, although the calculation of inductances and force by finite element analysis is covered extensively, (Bae, 2000). The design of longitudinal-flux, (Chappell, 1998; Lee, 2000; Bae *et al*., 1999; Lee *et al*., 1999) single-sided machines has been extensively studied, (Chappell, 1998) and procedures developed from these studies are presented in this section. A standard or classical design procedure begins with the power output equation relating the machine dimensions such as bore diameter, lamination stack length, speed, magnetic loading and electric loading. Further, the machine dimensions and their impact on performance are characterized by implicit relationships and made available in a form to enable machine design. Such a procedure allows insight into the scaling of designs and enables the exercise of engineering judgment to select the best design with the least amount of computations. These advantages are not feasible with finite element analysis; therefore, a standard design procedure is preferable for design of LSRM. To design an LSRM using a standard design procedure, analytical expressions relating machine dimensions to output variables are required. Recognizing that a standard design procedure is available for the rotary SRM, the design of an LSRM can proceed via the rotary SRM if the design specifications can be transformed from the linear to rotary domain and the design is then carried out in the rotary domain (D'hulster *et al*., 2004; Sheth and Rajagopal, 2003). The specifications can then be recovered in the linear domain by simple algebraic transformations.

LSRM CONFIGURATIONS

In this study, we will consider two longitudinal LSRM configurations: a three phase LSRM with an active stator and passive translator and a four-phase LSRM with an active translator and passive stator.

Three-phase lsrm with active stator and passive translator structure (D'hulster *et al*., 2004): Figure 1 shows the three-phase LSRM structure and its winding diagram with an active stator, a passive translator and a longitudinal flux configuration. The LSRM consists of six translator poles and n stator poles. This corresponds to the six stator/four rotor pole rotary SRM. One stator sector is composed of six stator poles and the number of stator sectors N_{sc}.

Corresponding Author: Cherif Fetha, Faculty of Sciences Engineering, University of Batna, Rue Chahid Med Elhadi Boukhlouf, 05000 Batna, Algeria

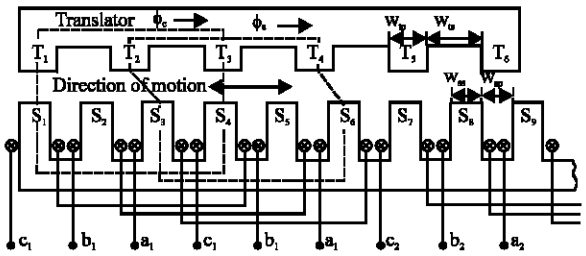

Fig. 1: Three-phase LSRM structure and winding diagram with six translator poles

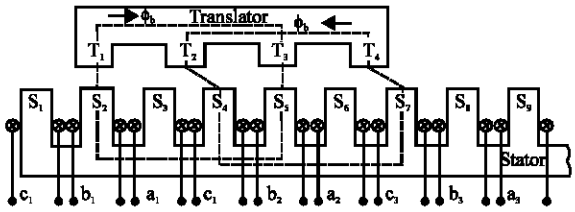

Fig. 2: Three-phase LSRM structure and winding diagrams with four translator poles

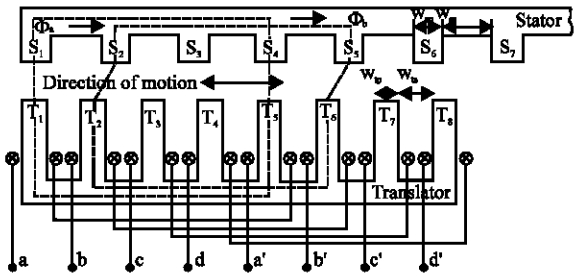

Fig. 3: Four-phase LSRM structure with active translator and passive stator

A rotary SRM has 4 rotor poles, hence the corresponding LSRM should have four translator poles. However, in the LSRM structure with four translator poles, there is a reversal of flux at the instant of phase current commutation. For example, consider the LSRM in Fig. 2, which has only four translator poles. For the continuous forward movement of LSRM, the excitation sequence of a_1a_2- b_1b_2-c_2c_3.... is necessary for motion in the increasing inductance region. However, this causes a flux reversal when the sequence is in between the excitation of b_1b_2-c_2c_3 and so on. This results in degradation of the LSRM performance with higher noise and increased core losses. If this topology is used, the converter design and the switching sequence are much more complicated. Therefore, the number of translator poles is increased from four to six to prevent the reversal of flux and to maintain the flux path in the same direction (Fig. 1). In the case of eight stator and six rotor poles in the rotary SRM, the number of translator poles should be increased from six to nine to maintain the flux in the same direction. The application of the sequence of c_1c_1' -a_1a_1'-b_1b_1' -c_2c_2'... makes the translator move in the forward direction continuously. The generated flux directions resulting from excitation of phase a and phase c windings are shown in Fig. 1. Each sector operates in an independent manner, which means that there is no simultaneous excitation of poles in different sectors. For example, the simultaneous excitation of $c_1'c_2$, $b_1'b_2$ and $a_1'a_2$ is not permitted. Therefore, there is no flux flow in the back iron between S_6 and S_7, hence the back iron portion between S_6 and S_7 can be used for other purposes such as stacking of laminations. As seen from Fig. 1, w_{tp} is the width of the translator pole, w ts is the width of the translator slot, w_{sp} is the width of the stator pole and w_{ss} is the width of the stator slot. The stacking width of the laminations is given by L_w.

Four-phase lsrm with active translator and passive stator structure: Figure 3 shows a four-phase longitudinal LSRM with an active translator and a passive stator. The LSRM consists of eight translator poles, corresponding to the eight stator and six rotor poles in the rotary SRM. Contrary to the active stator and passive translator structure, there is no reversal of flux at the instant of phase current commutation and the back irons of the stator and translator experience the same direction of magnetic flux regardless of the switching of the phase winding current.

The energization sequence of aa'-bb'-cc'-dd'-aa'-... in the increasing inductance region makes the translator move in the forward direction continuously with the flux direction maintained the same. The flux paths and directions for phase a and phase b excitation are shown in Fig. 3.

LSRM DESIGN, (Sheth and Rajagopal, 2003; Neagoe *et al.*, 1997; Haataja and Pyrhohnen, 2000)

The design of LSRM is achieved by first translating its specifications into equivalent rotary SRM specifications, then the rotary SRM is designed from which the LSRM dimensions and design variables are recovered by inverse translation. The design procedure is derived in this study.

Specifications of the LSRM: Consider an LSRM to be designed for a machine stator length L_t , with a maximum linear velocity of v_m and an acceleration time t_a required to reach the maximum velocity. The maximum mass of the translator is restricted to M_t . Figure 4 shows the required velocity profile of the LSRM. If the deceleration time t_d=t_a,

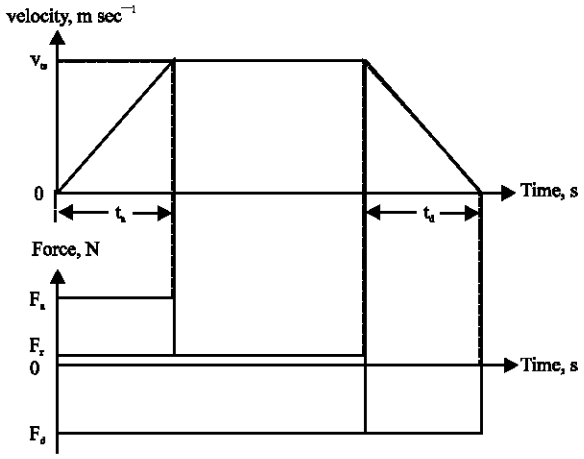

Fig. 4: Velocity and required force profile of LSRM

Design of rotary SRM: A 6/4 rotary SRM (RSRM) is designed for a power capacity identical to that of the LSRM. The material used for the laminations is M19 steel, which is made of non-oriented silicon steel. The rotary SRM has a stator pole angle of βs and a rotor pole angle of βr. The speed of the rotary SRM, N r , in rpm, (Lubin, 2002; Lilia, 2002).

The air gap of the LSRM is usually much larger than that of the air gap of the rotary SRM. In the aligned portion, the B-H characteristic of the magnetic material is fairly linear and the reluctance of the steel core is small when compared to the reluctance of the air gap in the aligned position. The machine flux can be calculated as: (Lee, 2000; Lubin *et al*., 2002; Lilia, 2002).

Conversion of RSRM dimensions to LSRM dimensions: The bore circumference of the rotary SRM forms the length of one sector of the LSRM. The total number of s ectors of the LSRM is given by Lee (2000) and Lee *et al*. (1999).

The winding details of the rotary SRM and LSRM are identical in this design. This need not be the case, as the duty cycle of a winding in the three-phase LSRM is $1/(3N_{sc})$, where as that of the rotary SRM winding is 1/3. Therefore, the windings in the LSRM can have much lower copper volume but take more losses.

NUMERICAL EXAMPLE

In this part contains two examples of the design procedure for a three-phase LSRM with an active stator and passive translator and a four-phase LSRM with an active translator and passive stator

Example 1: Design of three-phase LSRM with active stator and passive translator: An LSRM prototype is designed (Lee, 2000) for a length of 4.8 m, with a maximum linear velocity of 1,5 m sec^{-1} and acceleration time of 0,667 sec. The maximum mass of translator assembly is restricted to 20 kg. The acceleration is then given by:

$$a_a = \frac{v_m}{t_a} = \frac{1.5}{0.667} = 2.25 m/s^2$$

The force for initial acceleration is calculated as:

$$F_a = M_t.a_a = 20.2,25 = 45N$$

The deceleration a_d = -2.25 m sec^{-2} and the deceleration force F_d= - 45 N. The power capacity of the LSRM is:

$$P = F_a v_m = 45.1,5 = 67.5W$$

The rotary SRM is assumed to have a stator pole angle β_s= 30° = 0.524 rad and a rotor pole angle β_r=36° = 0.628 rad. After fine-tuning the parameters, the constants are set as follows: ke = 0.4 , k_d = 1, k_2 = 0.7, B = 1.1215 T, A_s=23886.5 and k=0.655. The bore diameter is obtained as:

$$D = \sqrt{\frac{P\pi}{60.k_e k_d k_1 k_2 k B A_s v_m}} = 76.39mn$$

The stack length of the rotary SRM is obtained as:

$$L = kD = 0.665.76.39 = 50mn$$

The stator yoke thickness b_{sy} is given by:

$$b_{sy} = \frac{D\beta_s}{2} = 20mn$$

Assuming D_o = 190 mm, the height of the stator pole, h_s, can be calculated as:

$$h_s = \frac{D_0}{2}\frac{D}{2} - b_{sy} = \frac{190}{2}\frac{76.39}{2} - 20 = 37mn$$

The rotor back iron width, b_{ry} and the height of the rotor pole (the translator pole), h_{rp}, are then calculated as:

$$b_{ry} = \left(\frac{D}{2}\right)\beta_r = \left(\frac{76.39}{2}\right)0.628 = 24mn$$

$$h_r = \frac{D}{2}l_g - b_{yr} = \frac{76.39}{2} - 1 - 24 = 15mn$$

The magnetic field intensity in the air gap is calculated as:

$$H_g = \frac{B}{\mu_0} = \frac{1.1215}{4\pi 10^{-7}} = 892461.3\ A/m$$

For a peak phase current of $I_p = 8.5$ A, the number of turns per phase is

$$T_{ph} = \frac{H_g.(2l_g)}{I_p} = 210\ \text{Turns/phase}$$

Assuming a current density of J = 6 A/mm2, the area of the conductor is calculated as:

$$a_c = \frac{I_p}{J\sqrt{q}} = \frac{8.5}{6\sqrt{3}} 0.818 mn^2$$

The closest wire size for this area of cross section of the conductor is AWG #18. It has an area of 0.817 mm^2 and is selected for the phase windings. The calculation of the winding turns completes the rotary SRM design. The conversion from rotary to linear domain follows.

The number of sectors of the LSRM and the resultant total number of stator poles are

$$N_{nc} = \frac{L_t}{\pi D} = \frac{4.8}{\pi.76,39.10^{-3}} = 20$$

$$n = P_s N_{sc} = 6.20 = 120$$

The width of the stator pole and the width of the stator slot are given by:

$$w_{sp} = \frac{D\beta_s}{2} = \frac{76.394.30\pi}{2.180} = 20mn$$

$$w_{ss} = \frac{(\pi D - 4w_{sp})}{4} = \frac{(\pi.76,394 - 6.20)}{4} = 20mn$$

The translator pole width and the translator slot width are calculated as:

$$w_{tp} = b_{yr} = 24mn$$

$$w_{ts} = \frac{(\pi D - 4w_{tp})}{4} = \frac{(\pi.76,394 - 4.24)}{4} = 36mn$$

The total length of the translator is given by:

$$L_{tr} = 6w_{tp} + 5w_{ts} = 6.24 + 5.36 = 324mn$$

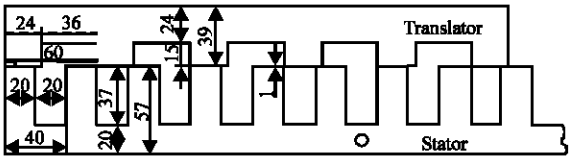

Fig. 5: Dimensions of the designed three-phase LSRM

The core stack width of the LSRM is obtained from the stator stack length of the rotary SRM as:

$$L_w = L = kD = 50mn$$

Now, the fill factor of the windings is verified to see if the slot size is sufficient to hold the windings. The diameter of the conductor is given by:

$$d_c = \sqrt{\frac{4.a_c}{\pi}} = \sqrt{\frac{4.0818}{\pi}} = 1.04mn$$

Assuming the width of the wedges w = 3 and packing factor $P_f = 0.8$, the number of vertical layers of winding and the number of horizontal layers of winding are obtained as:

$$N_v = P_f \frac{h_s - w}{d_c} = 0.8\frac{37-3}{1.02} = 26.15 \approx 26$$

$$N_h = \frac{T_{ph}}{2.N_v} = \frac{210}{2.26} = 4.03 \approx 4$$

The winding area is given by:

$$\text{Stator winding area} = 2\frac{a_c N_v N_h}{P_f} = 212,4mn^2$$

The fill factor is calculated as:

$$F_f = \frac{212.4}{(27-3).20} = 0.312$$

Finally, it can be observed that the condition outlined in Eq. 37 is satisfied with this design. Figure 5 shows the dimensions of the designed three-phase LSRM.
Unit: mm
Stack Length: 50
Coil: AWG #18. 210 Turns/Phase

Example 2: Four-phase LSRM prototype with active translator and passive stator: An LSRM prototype is designed51 for a length of 6 m, with a maximum linear velocity of 1 m sec^{-1} and acceleration time of 1.5 sec. The maximum mass of translator assembly is restricted to 60 kg. The acceleration is then given by:

$$a_a = \frac{v_m}{t_a} = \frac{1}{1.5} = 0.667 \text{m s}^{-2}$$

The instantaneous acceleration force is calculated as:

$$F_a = M_t.a_a = 60.0,667 = 40\text{N}$$

The deceleration a_d = -0.667 m sec^{-2} and the instantaneous deceleration force F_d=-40N. The power capacity of the LSRM is P=F_{avm}=40 W

The rotary SRM is assumed to have a stator pole angle β_s= 18° = 0.314 rad and a rotor pole angle βr = 22 °= 0.384 rad. After fine-tuning the parameters, the constants are set as follows:

k_e= 0.3 , k_d= 1, k_2= 0.7, B = 0.65 T, A_s= 41456.7 and k = 0.8

The bore diameter is obtained as:

$$D = \sqrt{\frac{P\pi}{60.k_e k_d k_1 k_2 kBA_s v_m}} = 75\text{mn}$$

The stack length of the rotary SRM is obtained as:

$$L = kD = 0,8.75 = 60\text{mn}$$

The stator yoke thickness b_{sy} is given by:

$$b_{sy} = \frac{D\beta_s}{2} \approx 12\text{mn}$$

Assuming D_0= S190 mm, the height of the stator pole h_s can be calculated as:

$$h_s = \frac{D_0}{2}\frac{D}{2} - b_{sy} = \frac{190}{2}\frac{75}{2} - 12 = 44\text{mn}$$

The rotor back iron width b_{ry} and the height of the rotor pole h_r are then calculated as:

$$b_{ry} = \left(\frac{D}{2}\right)\beta_r = \left(\frac{75}{2}\right)0,384 = 15\text{mn}$$

$$h_r = \frac{D}{2} - g - b_{ry} = \frac{75}{2} - 3 - 15 = 15\text{mn}$$

The magnetic field intensity in the air gap is calculated as:

$$H_g = \frac{\beta_g}{\mu_0} = \frac{0.65}{4\pi.10^{-7}} = 517253.6\text{A m}^{-1}$$

For a peak phase current of I_p = 8.5 A,

$$T_{ph} = \frac{H_g.(2g)}{I_p} = 360 \text{ turns/phase}$$

Assuming a current density of J = 6.5 A mm^{-2}, the area of the conductor is calculated as:

$$a_c = \frac{I_p}{J\sqrt{q}} = \frac{8.5}{6.5\sqrt{3}} = 0.654\text{mn}^2$$

AWG #19 wire size is suitable as it has an area of 0.653 mm^2.

In the active translator and passive stator structure of LSRM, the stator and rotor of the rotary SRM correspond to the translator and stator of LSRM, respectively.

The widths of stator pole and stator slot are given by:

$$w_{sp} = b_{ry} = 15\text{mn}$$

The total number of stator poles is

$$w_{ss} = \frac{(\pi D - 6w_{sp})}{6} = \frac{(\pi.75 - 6.15)}{6} = 25\text{mn}$$

The translator pole width and the translator slot width are calculated as:

$$w_{tp} = b_{sy} \approx 12\text{mn}$$

$$w_{ts} = \frac{(\pi D - 8w_{tp})}{8} = \frac{(\pi.75 - 8.12)}{8} = 18\text{mn}$$

The total length of the translator is given by:

$$L_{tr} = 8w_{tp} + 7w_{ts} = 8.12 + 7.1 = 222\text{mn}$$

The core stack width of the LSRM is obtained from the stator stack length of the rotary SRM as:

$$L_w = L = kD = 60\text{mn}$$

Now, the fill factor of the windings is verified to see if the slot size is sufficient to hold the windings. The diameter of the conductor is given by:

$$d_c = \sqrt{\frac{4.a_c}{\pi}} = \sqrt{\frac{4.0,654}{\pi}} = 0.912\text{mn}$$

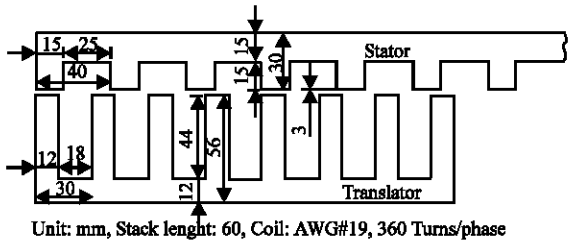

Fig. 6: Dimensions of the designed four phase LSRM

Assuming the width of the wedges w = 3 mm and packing factor P_f = 0.8, the number of vertical layers of winding and the number of horizontal layers of winding are given by:

$$N_v = P_f \frac{h_s - w}{d_c} = 0.8 \frac{44-3}{0.912} \approx 36$$

$$N_h = \frac{T_{ph}}{2.N_v} = \frac{360}{2.36} \approx 5$$

The winding area is given by:

$$\text{Stator winding area} = 2\frac{a_c N_v N_h}{P_f} = 293.9 \text{ mn}^2$$

The fill factor is calculated as:

$$F_f = \frac{\text{stator winding area}}{\text{stator slot window area}} = \frac{293.9}{3(44-3)} = 0.398$$

Note that the condition outlined is also satisfied with this design. Figure 6 shows the final dimensions of the designed four-phase LSRM.

CONCLUSION

The design verification process, very much similar to that for the rotary SRM, includes analytical and finite element analyses and experimental verification of the machine, (Lee, 2000). The analytical part of the verification is in finding the performance of the machine through its flux linkage vs. current vs. translator position characteristics derived using a magnetic equivalent circuit approach The finite element analysis is made using commercial software and the design is fine-tuned with these results. Then, the prototype is usually built and tested. A strong correlation between the analytical, finite element and experimental results assures confidence in the engineering analysis and the design method adopted and enables confident scaling of the machine. A poor correlation of the results forces the designer to revisit the design methodology.

REFERENCES

Bae, H.K., B.S. Lee, P. Vijayraghavan and R. Krishnan, 1999. A linear switched reluctance motor: Converter and Control. Conf. Rec. IEEE. Ind. Applied Soc. Ann. Mtg., pp: 547-554.

Bae, H.K., 2000. Control of switched reluctance motors considering mutual inductance, Ph.D. Thesis, The Bradley Department of Electrical and Computer Engineering, Virginia Technology, Blacksburg, VA.

Chappell, P.H., 1998. Current pulses in switched reluctance motor, IEEE. Proc. B, pp: 135.

D'hulster, F., K. Stockman, R.J.M. Belmans, 2004. Modelling of switched reluctance machines: State of the Art. IASTED., 24: 216-224.

Haataja, J. and J. Pyrhohnen, 2000. Synchronous reluctance motor: An alternative to induction motor, International Conference on Electrical Machines, ICEM, Espoo, Finland, pp: 1762-1766.

Lee, B.S., 2000. Linear Switched Reluctance Machine Drives with Electromagnetic Levitation and uidance Systems, Ph.D. Thesis, The Bradley Department of lectrical and Computer Engineering, Virginia Technology Blackburg, VA.

Lee, B.S., H.K. Bae, P. Vijayraghavan and R. Krishnan, 1999. Design of a linear switched reluctance machine, Conf. Rec. IEEE. Ind. Applied Soc. Ann. Mtg., pp: 2267-2274.

Lilia, E.L. AMRAOUI, 2002. Conception électromécanique d'une gamme d'actionneurs linéaire tubulaire à réluctance variable. Thèse de doctorat.

Lubin, T., H. Razik and A. Rezzoug, 2002. A new saturated model for synchronous reluctance machines. Proc. ICEM (CD-ROM), Brugge, Belgium.

Neagoe, C., A. Foggia and R. Krishnan, 1997. Impact of pole tapering on the electromagnetic torque of the switched reluctance motor, in IEEE Int. Electric Machines and Drives Conference, Milwaukee, WI.

Sheth, N.K. and K.R. Rajagopal, 2003. Optimum Pole Arcs for a Switched Reluctance Motor for Higher Torque With Reduced Ripple. IEEE. Trans. Mtg., pp: 3214-3216.